PAPER

# A new type of cyclotron resonance from charge-impurity scattering in the bulk-insulating $Bi_2Se_3$ thin films

IOP Publishing Journal of Physics D: Applied Physics
J. Phys. D: Appl. Phys. **55** (2022) 364004 (5pp) https://doi.org/10.1088/1361-6463/ac7a72

# A new type of cyclotron resonance from charge-impurity scattering in the bulk-insulating $Bi_2Se_3$ thin films

**Xingyue Han[1], Maryam Salehi[2], Seongshik Oh[3] and Liang Wu[1,*]**

[1] Department of Physics and Astronomy, University of Pennsylvania, Philadelphia, PA 19104, United States of America
[2] Department of Materials Science and Engineering, Piscataway, NJ, 08854, United States of America
[3] Department of Physics and Astronomy, Rutgers the State University of New Jersey, Piscataway, NJ 08854, United States of America

E-mail: liangwu@sas.upenn.edu

Received 12 April 2022, revised 3 June 2022
Accepted for publication 20 June 2022
Published 30 June 2022

**Abstract**

This work focuses on the low frequency Drude response of bulk-insulating topological insulator (TI) $Bi_2Se_3$ films. The frequency and field dependence of the mobility and carrier density are measured simultaneously via time-domain terahertz spectroscopy. These films are grown on buffer layers, capped by Se, and have been exposed in air for months. Under a magnetic field up to 7 Tesla, we observe prominent cyclotron resonances (CRs). We attribute the sharp CR to two different topological surface states from both surfaces of the films. The CR sharpens at high fields due to an electron-impurity scattering. By using magneto-terahertz spectroscopy, we confirm that these films are bulk-insulating, which paves the way to use intrinsic TIs without bulk carriers for applications including topological spintronics and quantum computing.

Keywords: topological insulator, cyclotron resonance, $Bi_2Se_3$

(Some figures may appear in colour only in the online journal)

## 1. Introduction

Ordered states of matter are usually characterized by Landau's spontaneous symmetry breaking theory. For example, ferromagnets break continuous rotation symmetry and superconductors break gauge symmetry. The newly discovered topological materials are classified by the topological properties of their bulk wavefunction. For example,the three-dimensional topological insulators (TIs) possess insulating bulk states and conducting surface states [1, 2]. Intrinsic bulk-insulating TIs are the ideal platforms for low-dissipation spintronics and quantum computing due to the spin-momentum locking on the topological surface states (TSSs) [1, 2]. However, most TI materials are slightly doped and thus have a conducting bulk, which is the major obstacle to reach the ideal TI state. To solve the problem, many attempts are made to tune the chemical potential toward the Dirac point. It was a success in graphene to probe many-body interactions with plasmons and phonons [3], and in Cu doped $Bi_2Se_3$ with dominating electron–phonon coupling [4]. More advancements in TIs are still lacking.

$Bi_2Se_3$ is a typical 3D TI with a single Dirac cone on the surface. However, native grown $Bi_2Se_3$ is known with a conducting bulk from defects. One way to suppress the bulk carrier density is the chemical doping method [5, 6]. However, the bulk carrier densities in these samples are still not negligible and the impurity states are pinned close to the chemical potential. The other way to suppress the bulk carriers is to grow $Bi_2Se_3$ on a buffer layer [7, 8]. An open question remains on how to keep the sample bulk-insulating after exposure in

* Author to whom any correspondence should be addressed.

 

air. In this work, we investigate $Bi_2Se_3$ thin films grown on a buffer layer with Se capping. The TSSs are decoupled via time-domain terahertz spectroscopy with a magnetic field up to 7 tesla.

Cyclotron resonance (CR) measurements have been shown very useful to study the Dirac fermions and many-body interactions [9–11]. It is also one of the most precise method to determine the carrier effective mass [12]. In previous work, $Bi_2Se_3$ films with conducting bulk showed a large Kerr rotation without obvious resonance [13]. In a later report, CR emerges in $In_2Se_3$ capped $Bi_2Se_3$ films [11] due to the destroyed non-TI/TI interface from Indium diffusion [14]. This is because a phase transition from topological to trivial insulator occurs at a low Indium concentration (∼6%) [15]. Besides, Cu doped $Bi_2Se_3$ films also presents CR, where the bulk-insulating state is reached and the electron–phonon coupling was revealed [4].

## 2. Results and discussion

Here we report time-domain THz spectroscopy measurement on $Bi_2Se_3$ thin films with 100 nm Se capping layer and $(Bi_{1-x}In_x)_2Se_3$ buffer layer (BIS-BL) [7]. These films have been exposed in air for 6 months. By using CR measurement, we confirm that these films are still bulk-insulating. We attribute the conducting channels to two different TSSs on the top and bottom of the films. By using magneto-terahertz spectroscopy, we observe that the CR sharpens at higher magnetic field, which reveal with long-range electron impurity scattering on the surfaces.

Figures 1(a) and (b) shows the real and imaginary conductance for 32QL and 16QL $Bi_2Se_3$ grown on BIS-BL at 5 K. The spectral weight is lower compared with the normal $Bi_2Se_3$ directly grown on sapphire or Si [13], even lower than the bulk-insulating $Cu_{0.02}Bi_2Se_3$ [4]. This indicates the bulk insulating behavior of the samples. The spectra can be fitted by the sum of (i) two Drude terms describing free electron-like motions from top and bottom surfaces respectively, (ii) a Drude–Lorentz term describing phonon oscillations, and (iii) a constant term counting for the background above the measured spectral range, as shown below.

$$G(\omega) = \epsilon_0 d\left(\sum_{i=1}^{2} -\frac{\omega_{pDi}^2}{i\omega - \Gamma_{Di}} - \frac{i\omega\omega_{pDL}^2}{\omega_{DL}^2 - \omega^2 - i\omega\Gamma_{DL}} - i(\epsilon_\infty - 1)\omega\right). \quad (1)$$

Here $\Gamma_{Di}$ and $\omega_{pDi}$ are the scattering rates and plasma frequencies of the $i$-th Drude term. $\Gamma_{DL}$ and $\omega_{pDL}$ are the scattering rate and plasma frequency of the Drude–Lorentz term. $d$ is the film thickness. $\epsilon_\infty$ is a constant named lattice polarizability. In the real part of the conductance $G_{D1}$, the total spectral weight ($\omega_{pD}^2 d$) can be extracted from the integral of each feature with a coefficient $\frac{\pi\epsilon_0}{2}$. This gives the ratio of the carrier density and the effective transport mass.

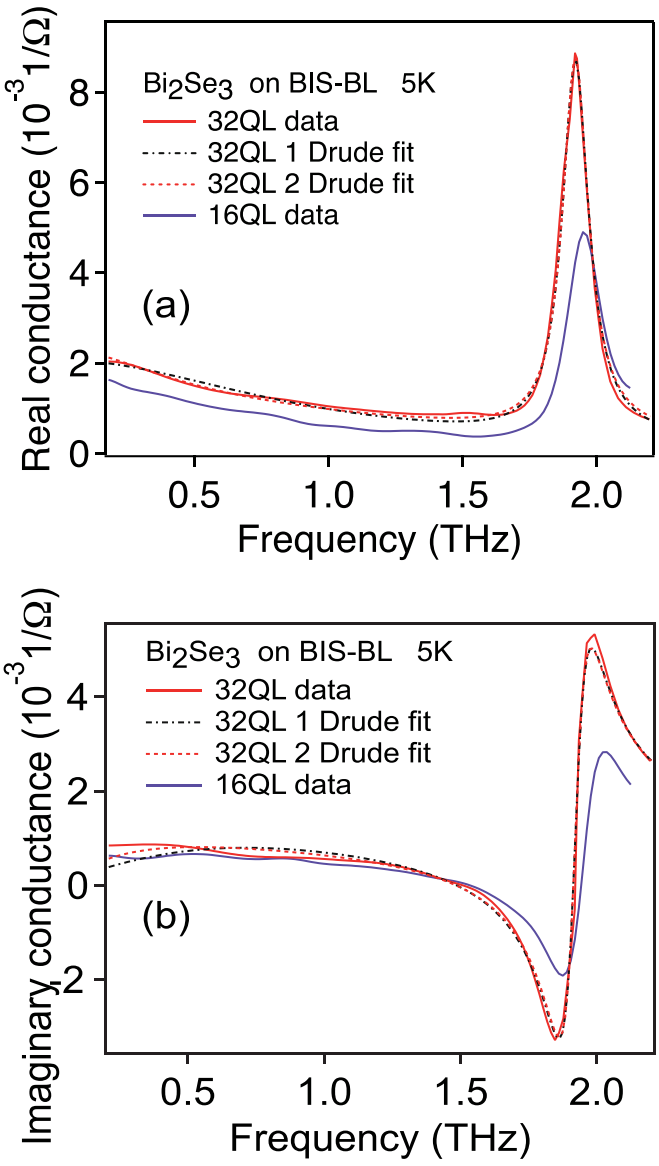


**Figure 1.** (a) Real and (b) imaginary conductance of 32QL and 16QL $Bi_2Se_3$ grown on BIS-BL at 5 K.

$$\frac{2}{\pi\epsilon_0}\int G_{D1}\,d\omega = \sum_{i=1}^{2}\omega_{pDi}^2 d = \sum_{i=1}^{2}\frac{n_{2Di}e^2}{m_i^*\epsilon_0}. \quad (2)$$

In the second equality, $n_{2Di}$ and $m_i^*$ are the carrier densities and the effective transport masses of the massless Dirac fermions. $m^*$ is defined as $m^* = \hbar k_F / v_F$. Consider a quadratic dispersion model for the TSS, $E = Ak_F + Bk_f^2$, the coefficients $A$ and $B$ can be obtained from photo-emission [4]. Then the last term in equation (2) can be expressed by $k_F$ only. For *one* surface state, the relation between spectral weight and $k_F$ is as following. Note that the right side of following expression is half of the value in the $Bi_2Se_3$ when we assume two nominally same TSSs were observed in $Bi_2Se_3$.

$$\omega_{pDi}^2 d = \frac{k_F(A + 2Bk_F)e^2}{4\,\pi\hbar^2\,\epsilon_0}. \quad (3)$$

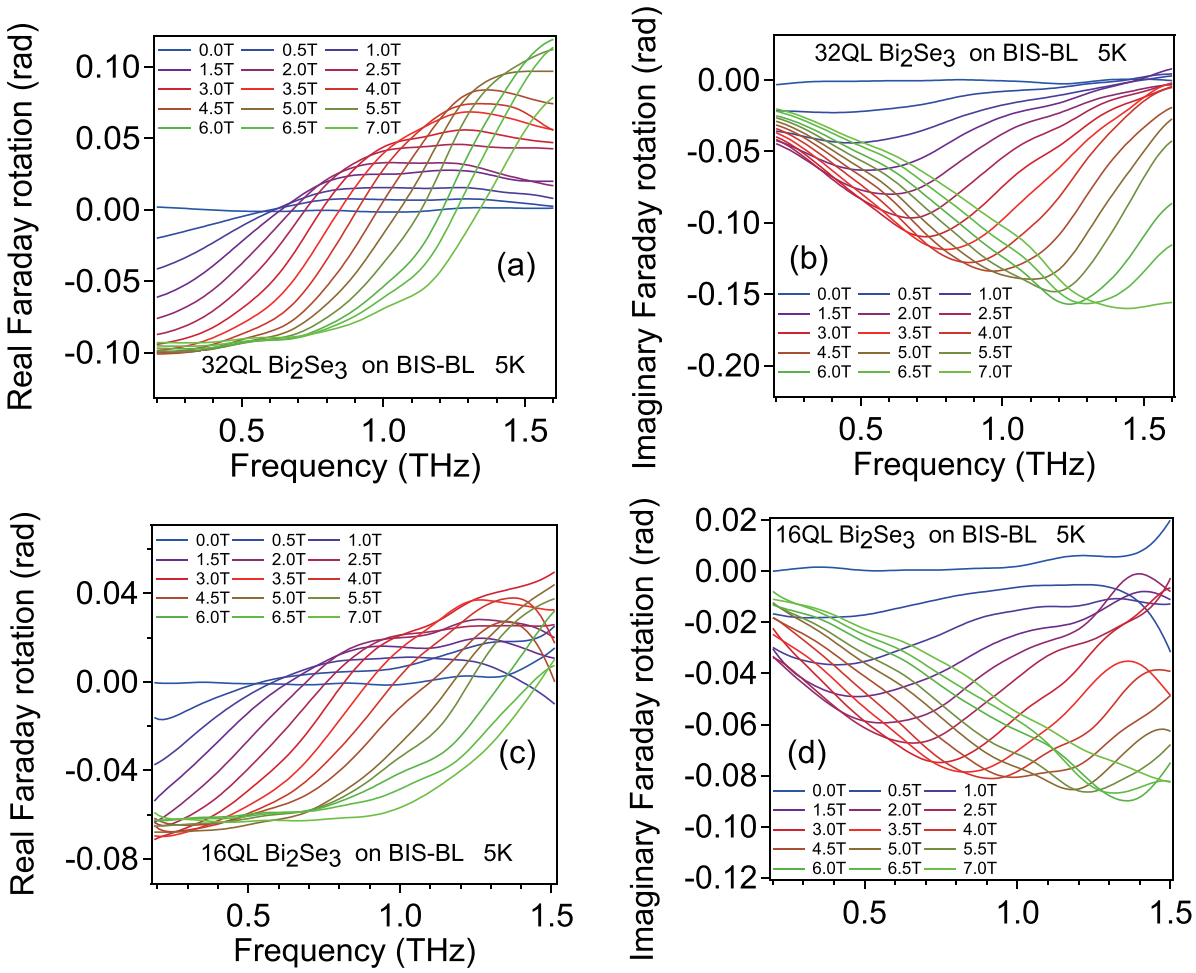


**Figure 2.** (a) Real part and (b) imaginary part of complex Faraday rotation for 32QL $Bi_2Se_3$ grown on BIS-BL layer. (c) Real part and (d) imaginary part of complex Faraday rotation for 32QL $Bi_2Se_3$.

At first, a single conduction channel originated from two identical TSSs is assumed. Using equations (2) and (3), the $n_{2D}$ and m$^*$ can be determined. The fitting results of the 32QL sample gives a *total* sheet carrier density $n_{2D} \sim 4.8 \times 10^{12}$ cm$^{-2}$, effective transport mass $m^* \sim 0.135$ ($\pm 0.005$) $m_e$, Fermi energy $E_F \sim 140$ ($\pm 10$) meV, and phonon frequency $\omega_{ph} \sim 1.92$ THz. 16QL sample has lower spectral weight than 32QL sample. The same analysis gives a *total* sheet carrier density $n_{2D} \sim 3.8 \times 10^{12}$ cm$^{-2}$, $m^* \sim 0.12$ ($\pm 0.005$) $m_e$, $E_F \sim 120$ ($\pm 8$) meV and phonon frequency $\omega_{ph} \sim 1.95$ THz. The estimation of the chemical potential is consistent with an insulating bulk even after exposure in air for 6 months [7].

We performed Faraday rotation measurements on these samples to measure the CR mass and spectral weight. Data are shown in figures 2(a)–(d). Similar to $Cu_{0.02}Bi_2Se_3$, cyclotron resonates are observed in both 32QL and 16QL samples. We use the following model to fit the conductance spectra under an external magnetic field. Here we assume two equal contribution from top and bottom surface states (bSSs):

$$G_{\pm} = -i\epsilon_0\omega d\left(\sum_{i=1}^{2}\frac{\omega_{pDi}^2}{-\omega^2 - i\Gamma_{Di}\omega \mp \omega_c\omega} + \frac{\omega_{pDL}^2}{\omega_{DL}^2 - \omega^2 - i\omega\Gamma_{DL}} + (\epsilon_\infty - 1)\right). \quad (4)$$

Here the $\pm$ sign corresponds to the right/left-hand circularly polarized light, respectively. $\omega_c$ is the CR frequency. The Faraday rotation can be expressed by $\tan(\theta_F) = -i(t_+ - t_-)/(t_+ + t_-)$. Here we let $\omega_c$ and $\Gamma_D$ vary with field. We find that the fit result is not good as shown in figure 3(a). Let us further address the 1 Drude model analysis. As we can see in figure 3(a), the fit quality of 1 Drude term is not as good as $Cu_{0.02}Bi_2Se_3$ case. $Bi_2Se_3$ is grown on $(Bi_{1-x}In_x)_2Se_3$, and $\leqslant 0.2\%$ In is diffused into the bottom $Bi_2Se_3$ few layers. Even though 0.2% is far below the topological phase transition threshold [15], it is natural to treat top surface states (tSSs) and bSSs differently. We remove the equal contribution from both surface states and treat them separately as equation (4). The fit quality improve significantly as shown in figure 3(a). We can also see two Drude

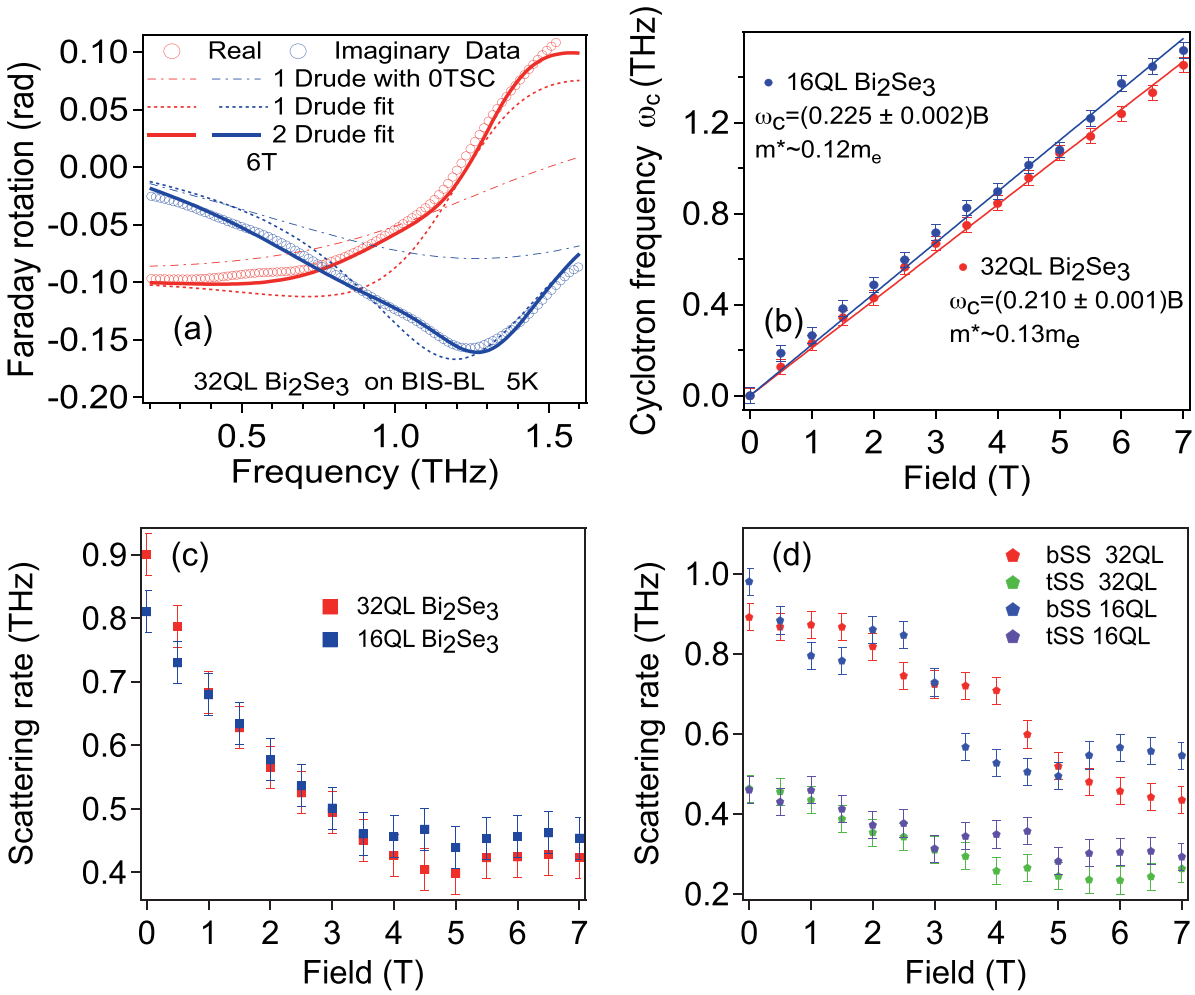


**Figure 3.** (a) A representative fit quality for 1 Drude fit (dashed line) and 2 Drude fit (solid line) and a calculation by using zero-field scattering rate (0TSC) of 32QL sample. (b) Cyclotron frequency VS field from 1 Drude fit. Solid line is linear fit. Drude scattering rate VS field from (c)1 Drude fit. (d) 2 Drude fit.

**Table 1.** Fit parameters for two-Drude fit.

| | $n_{2D}$ ($10^{12}$ cm$^{-2}$) | m$^*$ ($m_e$) | $\Gamma$(7 T) (THz) | $\mu$(7 T) (cm$^2$ V$^{-1}$ s$^{-1}$) |
|---|---|---|---|---|
| tSS 32QL | 2.2 | 0.13 | 0.24 | 8980 |
| bSS 32QL | 2.7 | 0.14 | 0.55 | 3640 |
| tSS 16QL | 1.3 | 0.11 | 0.29 | 8780 |
| bSS 16QL | 2.0 | 0.12 | 0.43 | 5420 |

terms fit zero-field conductance better in figure 1. Then we can extract carrier density of each surface state by the relation $\omega_{pDi}^2 d = \frac{n_{2Di}e^2}{m_i^* \epsilon_0}$. The parameters for two Drude fits are showed in table 1. Indium causes more scattering and therefore the channel with larger scattering rate is identified as bSS. As shown in previous works, the bottom surface has more defects, which lead to higher carrier density [7, 13]. Therefore, the large scattering rate and the large carrier density are consistent with each other for the bottom surface. We also performed Faraday rotation measurements on bare buffer layer and no rotation angle is observed. So the CR feature comes from the $Bi_2Se_3$ sample only.

Now let us address the decreasing scattering rate VS field as shown in figures 3(c) and (d). Short-range charge impurity scattering rate leads to $\sqrt{B}$ increasing scattering rate, as predicted and observed in graphene [16–18]. Electron–phonon scattering rate causes broadening of CR and saturation of scattering rate above phonon energy [4]. Long-range charge impurity scattering rate leads to decreasing scattering rate VS field [19]. It was not the dominant mechanism in graphene and therefore was never observed. Similar trend were reported in InSe quantum well and was interpreted as scattering over Gaussian potential larger or equal to the cyclotron orbit [20]. The saturation of scattering rate above 4 T in figures 3(c) and

(d) is due to electron–phonon scattering as cyclotron frequency reaches ∼0.7 THz at 4 T in both samples which corresponds to either Kohn anomaly of surface $\beta$ phonon or highest acoustic phonon frequency [4]. In the two-Drude fit, one channel has stronger field dependence and is identified as bSS. The reason is charge impurities most likely are created on the bSS due to charge imhomogenity. TSS has less effect due to screening. This kind of long-range charge impurity scattering was further corroborated by the fact no Shubnikov de-Has (SdH) oscillation was observed on these sample while CR is very robust [7]. SdH is limited by quantum life-time which is sensitive to both small-angle and large-angle scatting while CR is sensitive to transport life-time which is limited by back scattering. The low quantum life-time in these samples indicates significant small-angle scattering rate coming from long-range coulomb potential. Similar trend was observed in 2DEG system [21] and theoretically investigated in literature [22].

To conclude, we observe sharp CR in bulk-insulating $Bi_2Se_3$ thin films. The field dependence reveals a decreasing of the scattering rate with increasing magnetic fields. We attribute the origin to impurity scattering due to the buffer layer. This work shows that CR is a powerful tool to study many-body interactions in topological materials. On the practical side, this work establishes that a 100 nm thick Se capping layer is simple, but very useful for keeping the TI thin films bulk-insulating. The evidence for the long-range impurity scattering at the bottom interface due to buffer layers shreds light on film growth to further decreases the carrier concentration and enhances mobility for future low-dissipation spintronic devices.

## Data availability statement

The data that support the findings of this study are all present in this paper. Further data are available from the corresponding author upon reasonable request.

## Acknowledgments

This project is supported from the ARO under the Grant W911NF2020166. The development of the THz polarity is supported by the ARO YIP award under the Grant W911NF1910342. The acquisition of the laser for the THz system is support from a seed grant at National Science Foundation supported University of Pennsylvania Materials Research Science and Engineering Center (MRSEC)(DMR-1720530). X H is also partially supported by the Gordon and Betty Moore Foundation's EPiQS Initiative, Grant GBMF9212 to L W . L W also acknowledges partial summer support from the NSF EArly-concept Grants for Exploratory Research (EAGER) grant (Grant No. DMR2132591).

## ORCID iD

Xingyue Han https://orcid.org/0000-0001-6775-4171

## References

[1] Hasan M Z and Kane C L 2010 *Rev. Mod. Phys.* **82** 3045
[2] Qi X-L and Zhang S-C 2011 *Rev. Mod. Phys.* **83** 1057
[3] Basov D, Fogler M, Lanzara A, Wang F and Zhang Y 2014 *Rev. Mod. Phys.* **86** 959
[4] Wu L, Tse W-K, Brahlek M, Morris C M, Aguilar R V, Koirala N, Oh S and Armitage N P 2015 *Phys. Rev. Lett.* **115** 217602
[5] Ren Z, Taskin A A, Sasaki S, Segawa K and Ando Y 2010 *Phys. Rev.* B **82** 241306
[6] Xiong J, Petersen A, Qu D, Hor Y, Cava R and Ong N 2012 *Physica* E **44** 917
[7] Koirala N *et al* 2015 *Nano Lett.* **15** 8245
[8] Wu L, Salehi M, Koirala N, Moon J, Oh S and Armitage N 2016 *Science* **354** 1124
[9] Crassee I, Levallois J, Walter A, Ostler M, Bostwick A, Rotenberg E, Seyller T, Van Der Marel D and Kuzmenko A 2011 *Nat. Phys.* **7** 48
[10] Jiang Z, Henriksen E, Tung L, Wang Y-J, Schwartz M, Han M, Kim P and Stormer H 2007 *Phys. Rev. Lett.* **98** 197403
[11] Jenkins G S, Schmadel D C, Sushkov A B, Drew H D, Bichler M, Koblmueller G, Brahlek M, Bansal N and Oh S 2013 *Phys. Rev.* B **87** 155126
[12] Kono J and Miura N 2006 *High Magnetic Fields: Science and Technology* vol III (Singapore: World Scientific)
[13] Valdés Aguilar R *et al* 2012 *Phys. Rev. Lett.* **108** 087403
[14] Lee H, Xu C, Shubeita S, Brahlek M, Koirala N, Oh S and Gustafsson T 2014 *Thin Solid Films* **556** 322
[15] Wu L, Brahlek M, Aguilar R V, Stier A V, Morris C M, Lubashevsky Y, Bilbro L S, Bansal N, Oh S and Armitage N P 2013 *Nat. Phys.* **9** 410
[16] Shon N H and Ando T 1998 *J. Phys. Soc. Japan* **67** 2421
[17] Orlita M *et al* 2008 *Phys. Rev. Lett.* **101** 267601
[18] Jiang Z, Henriksen E, Tung L, Wang Y-J, Schwartz M, Han M, Kim P and Stormer H 2007 *Phys. Rev. Lett.* **98** 197403
[19] Yang C, Peeters F and Xu W 2010 *Phys. Rev.* B **82** 075401
[20] Kress-Rogers E, Nicholas R and Chevy A 1983 *J. Phys. C: Solid State Phys.* **16** 2439
[21] Gaska R, Yang J, Osinsky A, Chen Q, Khan M A, Orlov A, Snider G and Shur M 1998 *Appl. Phys. Lett.* **72** 707
[22] Adam S, Hwang E and Sarma S D 2012 *Phys. Rev.* B **85** 235413